GEOFIZIKA VOL. 22 2005

Original scientific paper
UDC 551.465

Turbulent mixing in the springtime central Adriatic Sea

Hartmut Peters[1] and Mirko Orlić[2]

[1] Rosenstiel School of Marine and Atmospheric Science, University of Miami, Miami, USA

[2] Department of Geophysics, Faculty of Science, University of Zagreb, Zagreb, Croatia

Received 11 March 2005, in final form 25 June 2005

A small set of observations of upper ocean turbulent mixing, stratification and currents was obtained in the central Adriatic Sea in May 2003. Owing to light winds, the surface mixed layer was at most 10 m thick and usually much thinner. The water column below was mostly strongly stratified with partially restratified remnant of previous mixed layers. Mesoscale currents were weak with a significant barotropic component. Weak shear and strong stratification tended to combine to large Richardson numbers. Below a layer of enhanced mixing in the upper 10–20 m, eddy diffusivities were mostly small, ranging from 10^{-6} m^2 s^{-1} to about 5×10^{-5} m^2 s^{-1}. Much larger values occurred in a few events, however.

Keywords: microstructure, turbulence, Adriatic

1. Introduction

While it appears to be widely accepted that turbulent mixing is an important part of the ocean circulation, it still is the least understood component. And although direct observations of mixing have become increasingly common since oceanic microstructure measurements matured to a »production« tool in the early 1980s, they are still being made far less frequently than conventional hydrographic and current measurements. With this background, it appears worthwhile to report herein one of the first direct observations of ocean mixing in the central Adriatic Sea even though the set of measurements is small as a result of the loss of the core instrumentation less than two days out of port.

Previously published studies of the Adriatic mixing were limited to the determination of eddy diffusivities by fitting some simple models to data. Schmidt (1917) and Gačić (1972) related a one-dimensional heat diffusion equation to vertical profiles of temperature repeatedly taken at a station. Saint-Guily (1965) and Malačič (1991) minimized the difference between an analytical solution of the heat diffusion equation and observed annual cycle

of temperature. On the other hand, Zore-Armanda (1963) combined a theoretical result previously obtained by Jacobsen (1927) with *TS* diagrams successively recorded at a station. Finally, Supić et al. (1997) and Grbec and Morović (1997) assumed continuity of heat flux across the sea surface and utilized estimates of the air-sea heat flux as well as vertical temperature gradients measured at the sea surface. For the springtime central Adriatic this resulted in widely differing eddy diffusivities of heat: according to Gačić (1972) they range between 8 and 58×10^{-4} m^2 s^{-1} along the vertical, following Grbec and Morović (1997) they are close to 2×10^{-4} m^2 s^{-1} at the sea surface.

The present paper simply describes the observations, which are introduced in Section 2 along with our methods for their analysis. Brief characterizations of the oceanic conditions in the central Adriatic during the time of the measurements near the end of May, 2003, follow. These address surface forcing, ocean currents and stratification. Thereafter the oceanic mixing is discussed in Section 4. For better readability of the paper detail of the data reduction and an assessment of uncertainties are relegated to the Appendix.

2. Observations and Flow Variables

The observations analyzed herein were made as part of the international DOLCEVITA project – Dynamics Of Localized Currents and Eddy Variability In The Adriatic. A first cruise within the project had taken place in the northern Adriatic in January/February 2003 under wintertime conditions and repeated bora wind events (Lee et al., 2005). Turbulence observations from this cruise will be analyzed elsewhere. A second set of cruises followed in late spring under very different environmental conditions. Extensive observations of stratification, currents and optical and biological parameters were made from the *R/V Knorr*. In parallel with the *Knorr* cruise, we observed turbulent mixing from the *R/V G. Dallaporta*. Her cruise track is depicted in Fig. 1, and stations are listed in Table 1.

Table 1. Stations of the R/V G. Dallaporta DOLCEVITA-2 cruise with number of CTD and microstructure profiles taken. Positions are nominal. Station depths are from the ADCP; for Stations 1–3 see Fig. 1.

Station	Time (UTC)	Latitude	Longitude	Depth (m)	CTD drops	SWAMP drops
1	27-May-03, 0829–1154	43°32.1'N	14°02.6'E		1	4
2	27-May-03, 1708–1727	43°04.9'N	15°04.7'E		0	3
3	27-May-03, 2204–2230	43°15.4'N	14°14.6'E		0	8
4	28-May-03, 0224–0306	43°35.0'N	15°26.6'E	177	0	10
5	28-May-03, 0753–0830	43°43.8'N	15°08.1'E	96	8	0
6	28-May-03, 1154–1224	43°34.3'N	14°57.8'E	101	0	7

The stratification was observed on station with a regular SeaBird 911+ CTD and with the CTD component of the Shallow Water Microstructure Profiler (SWAMP; Peters, 1997), which also employed SeaBird sensors. Ocean currents were observed on station and while steaming in between stations at 6 kn with a RD Instruments 300-kHz Workhorse acoustic Doppler current profiler (ADCP) towed over the stern of the *Dallaporta*. While drifting on station we took multiple SWAMP or CTD »drops«.

Stratification and current data are evaluated in terms of temperature (T), potential temperature (Θ), salinity (S), density (ρ), potential density (σ_θ), buoyancy frequency (N), east (u) and north (v) velocity components or speed (V) and direction (Φ), shear ($V_z = [(\partial u/\partial z)^2 + (\partial v/\partial z)^2]^{1/2}$), and gradient Richardson number ($Ri = N^2 V_z^{-2}$).

The microstructure section of SWAMP employed two shear probes, a fast FP07 thermistor, and a SeaBird dual needle micro-conductivity probe, all sampled at 256 Hz. As detailed in the Appendix, these measurements are analyzed in terms of the viscous dissipation rate ε and the thermal dissipation rate χ (Gregg, 1987). Following the Osborn-Cox method (Osborn and Cox, 1972), an eddy diffusivity of heat can be estimated from χ and the vertical temperature gradient:

$$K_h = \frac{1}{2}\chi\left(\frac{\partial T}{\partial z}\right)^{-2}. \tag{1}$$

Winters and D'Asaro (1996) show that the Osborn-Cox method is rigorously valid in a volume-average sense. In the following we use K_h as the primary measure of the »intensity« of turbulent mixing. Similarly, following Osborn (1980), an eddy diffusivity of mass can be estimated from ε and N^2 assuming a constant flux Richardson number,

$$K_\rho = 0.2\,\varepsilon\,N^{-2}. \tag{2}$$

The value of 0.2 for the mixing efficiency is customary but subject to uncertainty and variability. This mixing efficiency and the Osborn method in general are further discussed, *e.g.*, by Gregg (1987), Yamazaki and Osborn (1993), Moum (1996), Smyth et al. (2001), and Baumert and Peters (2000). Peters et al. (1988) show that K_ρ and K_h track each other closely over a wide range from weak to strong mixing.

As an additional turbulence characteristic we present the buoyancy Reynolds number, $Re_b = \varepsilon/(\nu N^2)$, where ν is the kinematic viscosity. Re_b has been used as an indicator of the »activity« of turbulence. Following Gargett et al. (1984), Gregg (1987), and Rohr et al. (1988), active mixing sustaining a vertical buoyancy flux requires $Re_b \geq 20$, turbulence becomes isotropic for $Re_b \geq 200$ and exhibits fully universal character at $Re_b \geq 4 \times 10^4$. We note that Re_b is nei-

ther an ordinary flow Reynolds number nor a 1:1 substitute for a turbulent Reynolds number (Gregg, 1987; Peters et al., 1995).

Auxiliary data used herein include meteorological time series routinely collected at Šibenik and moored current time series taken at Stations A and B indicated in Fig. 1. The latter measurements were performed with bottom-mounted 300-kHz ADCPs within the framework of the East Adriatic Coastal Experiment (EACE; Orlić, 2003).

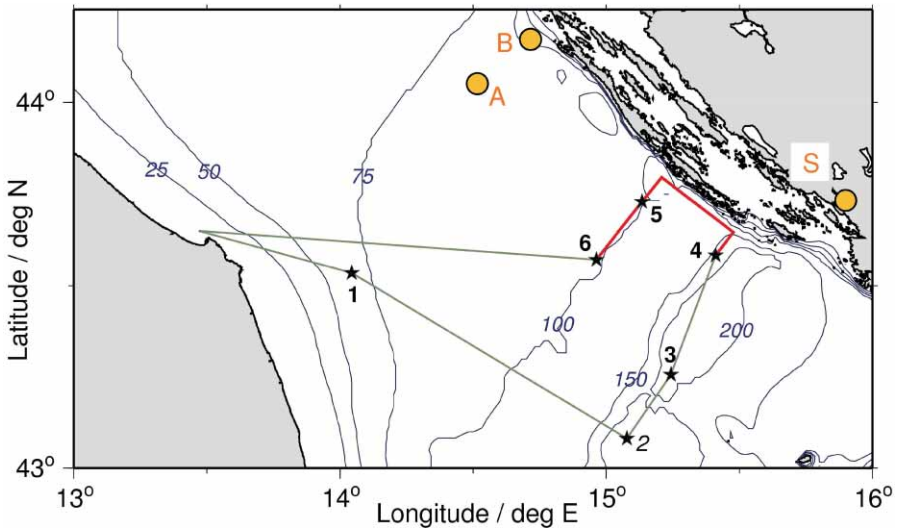

Figure 1. Station map of the DOLCEVITA-2 cruise of the *R/V G. Dallaporta*. Station numbers are indicated in bold numbers, while smoothed depth contours in meters are labeled in italics. An ADCP was towed from Station 4 to Station 6. Moored current measurements took place at locations »A« and »B;« winds were measured at Šibenik (»S«).

3. Surface Forcing, Currents and Stratification

a. Surface Forcing

Hourly wind vectors measured at Šibenik before and during the *Dallaporta* cruise are shown in Fig. 2a. There were two wind episodes during the interval considered, a stronger one on 21–23 May and a weaker on 28–29 May. Both were characterized by a considerable along-basin wind variability, and, in particular, operational mesoscale meteorological model run by the Hydrometeorological Institute of the Republic of Croatia revealed that during the second episode winds were stronger in the vicinity of Šibenik and EACE stations, weaker in between – close to our stations. However, no wind data were available for our measurement area. The first of the wind episodes was related to a cyclone which swept over the Adriatic on 21 May, the second

to the along-Adriatic air-pressure gradient which was established by 28 May. Between the two episodes the winds were weak, dominated by coastal breezes which developed in an almost uniform air-pressure field. Some precipitation was recorded at Šibenik on 20–21 May and again on 27–28 May, whereas air temperatures varied between 15 and 30 °C – with a considerable diurnal signal being visible in the data.

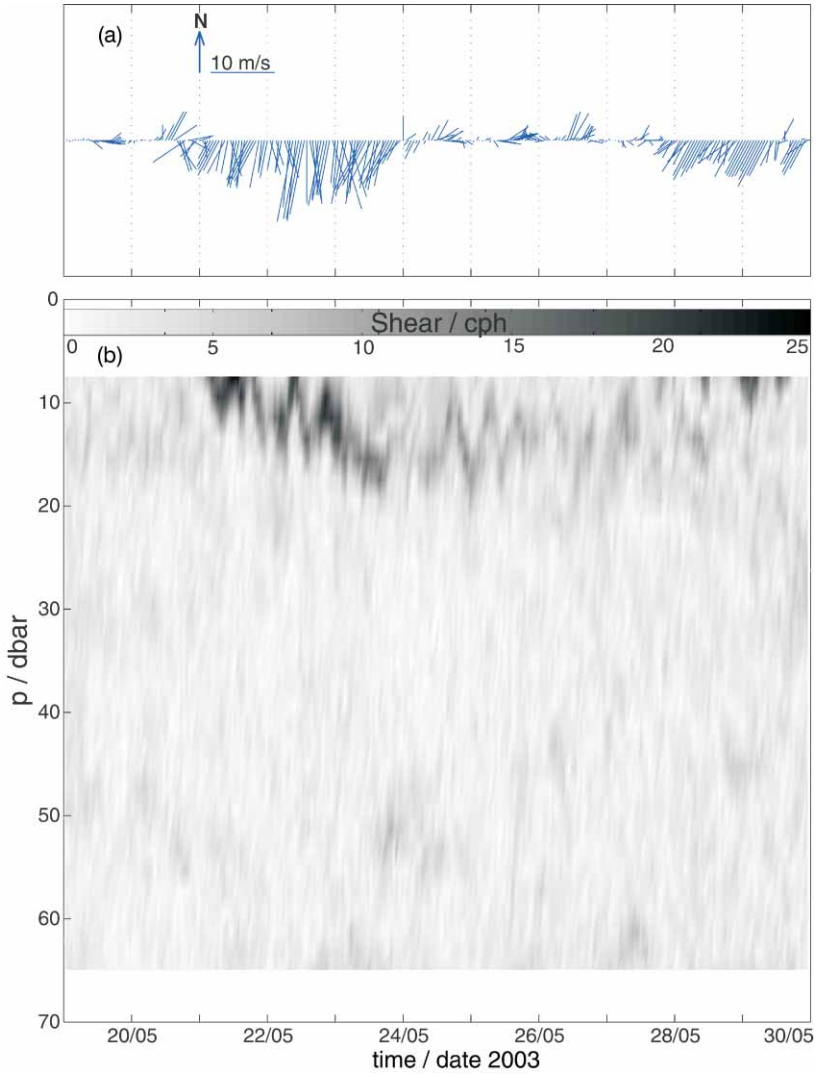

Figure 2. Hourly wind data taken at Šibenik (a) and hourly current shear (V_z as defined in the text) recorded at Station A with a 2-m vertical resolution (b). Fig. 1 shows the locations of these measurements.

b. Stratification, Shear and Richardson Numbers

Corresponding to a surface forcing characterized by weak winds over our measurement area, the upper 70–100 m of the Adriatic were mostly strongly stratified as shown in station summary profile plots of Figs. 3–8. These depict the mean from all drops taken at any one station. The deepest observed surface mixed layers of about 10 m occurred in Station 3 (Fig. 5), which was taken at night, and hence presumably under conditions of oceanic heat loss and mixed layer convection. Otherwise, the surface mixed layer was at most a few meters deep. However, remnants of deeper previous mixed layers, now partially restratified, occurred in Stations 1–3 (Figs. 3a–5a), the deepest with 30 m in Station 2. The strongest stratification observed with $N > 20$ cph (cycles per hour) occurred at shallow depths at the bottom of active or previous mixed layers. Otherwise typical values of N decreased from near 10 cph to 4 cph with depth over the top 70 m (Figs. 3b–8b). *TS* relationships tended to be complex owing to a highly variable $S(z)$, z being depth and numerically close to pressure *(p)* in dbar. Inversions in $T(z)$ were less prominent than those of $S(z)$ but occurred frequently nevertheless.

Our test station, Station 1 (Fig. 3 and Table 1), shows a highly mixed layer below 58 m depth. Our operations not having been established fully, we do not know the exact water depth at Station 1, and we also lack high-resolu-

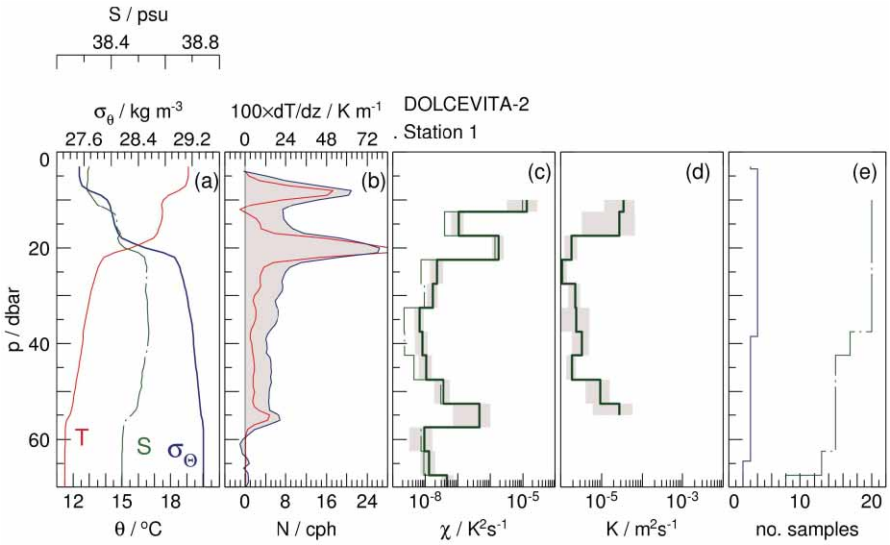

Figure 3. Mean Station 1 profiles: stratification (a) θ, S, σ_θ and (b) buoyancy frequency *(N,* shaded) and temperature gradient; (c) thermal dissipation rate (χ, with bootstrap confidence limits shaded) and uncorrected χ (dash-dotted, as explained in the text); (d) eddy diffusivity of heat *(K_h,* with bootstrap confidence bounds shaded); (e) number of sample: drops (solid) and number of χ data per 5-m bin (dash-dotted).

tion bathymetric data from the area. However, the descending SWAMP had not hit bottom at 77 m, its maximum depth during the drop. A depth greater than 77 m contrasts with the coarse bottom topography depicted in Fig. 1, which would indicate a water depth near 65 m. This suggests that the deep mixed layer of Station 1 exists in a local deep hole in the sea floor filled with a remnant of North Adriatic Dense Water formed during the previous winter (Vilibić et al., 2004).

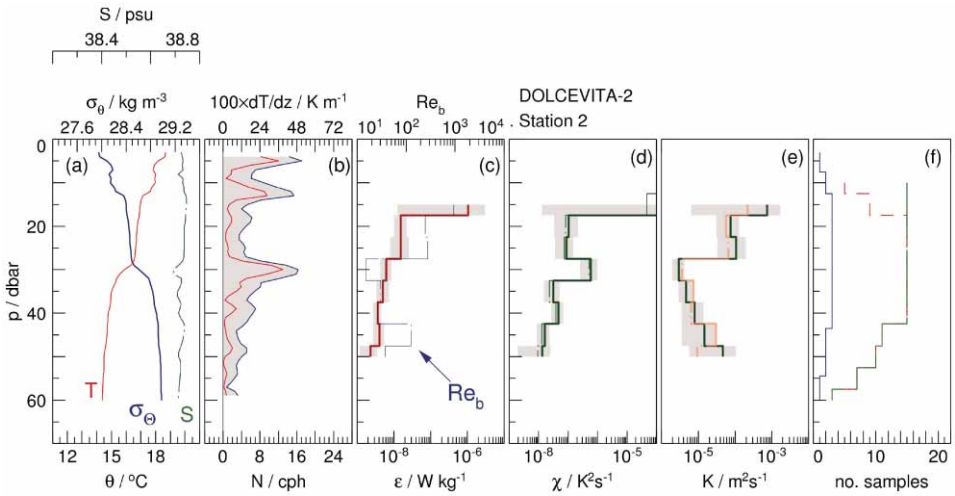

Figure 4. Mean Station 2 profiles: as Fig. 3 except (c) viscous dissipation rate (ε with bootstrap confidence bounds shaded) and buoyancy Reynolds number (Re_b, dash-dotted, light); (d) χ as in Fig. 3c; (e) K_h as in Fig. 3d with eddy diffusivity of mass added (K_ρ, dash-dotted, pink/light); (f) as Fig. 3e with number of samples of ε added (dashed).

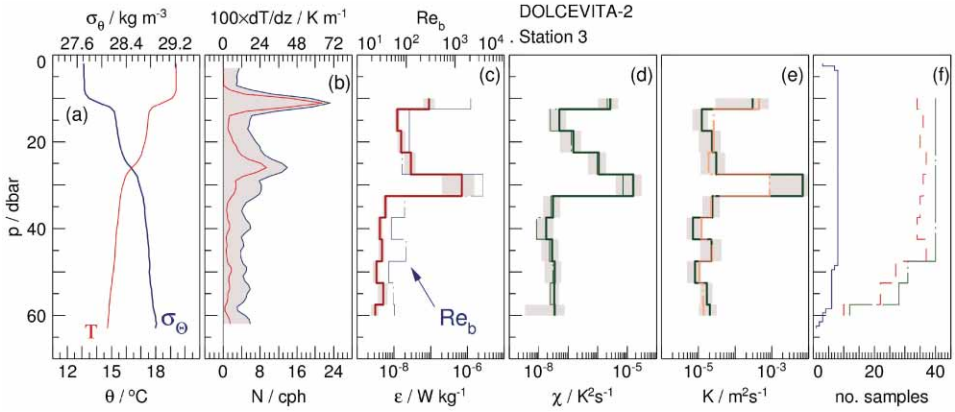

Figure 5. Mean Station 3 profiles: see Fig. 4.

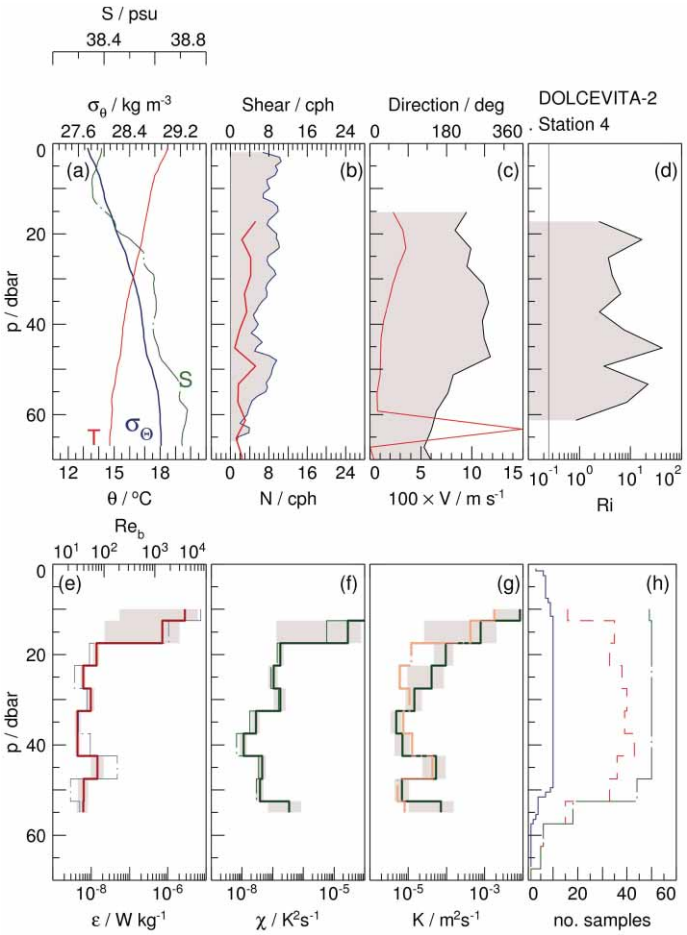

Figure 6. Mean Station 4 profiles: (a) stratification as in Fig. 4a; (b) N (shaded) and shear ($V_z = [(\partial u/\partial z)^2 + (\partial v/\partial z)^2]^{1/2}$); (c) current speed ($V$, shaded) and direction; (d) gradient Richardson number; (e) ε and Re_b as in Fig. 4c; (f) χ as in Fig. 4d; (g) K_h and K_ρ as in Fig. 4e; (h) number of samples as in Fig. 4f.

Stratification and shear combined indicate a potential for turbulent mixing. All individual estimates of N from the *Dallaporta* CTD and SWAMP have been replotted in Fig. 9, which shows great scatter in the upper 25 m and a decreasing trend with increasing depth. Because of the spatial separation the values of N can only in a very loose sense be compared with hourly shear values from the A and B EACE moorings shown in Fig. 10. Fig. 10 covers the time interval extending from 8 h UTC on 27 May to 12 h UTC on 28 May, *i.e.* simultaneously with our shipborne measurements. At Station A there was a maximum of shear close to the surface and an increase at depths

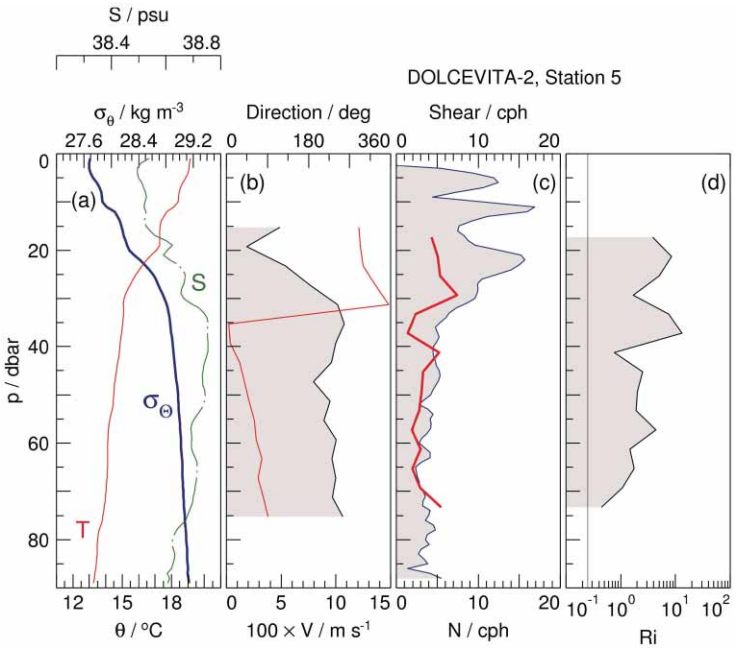

Figure 7. Mean Station 5 profiles, stratification from the SeaBird CTD: as Fig. 6a-d.

greater than 50 m, at Station B maximum occurred between 20 and 30 m. Obviously, the two stations were subjected to different current regimes, and that experienced by the *Dallaporta* was probably yet different. Nevertheless, we note that, while the *Dallaporta N* dropped below 5 cph at depths exceeding 60 m, some higher shear data occurred at mooring A.

A closer look at the time series of shear at Station A (Fig. 2) is revealing. Larger values were observed only close to the sea surface during the wind episodes, and at depths of 10–20 m between 24 and 27 May when the wind influence was unimportant. It is interesting to notice that the position of the shear maximum was oscillating during calm weather conditions – obviously due to the presence of internal waves. Their period is, however, difficult to determine from available data. Similar results were obtained for Station B (not shown), except that the shear was generally smaller and its maximum during the calm weather was located deeper and was oscillating with greater amplitudes.

Co-located shipborne measurements of shear and stratification indicate that gradient Richardson numbers generally stayed well above the linear stability threshold of 1/4 (Figs. 6b–8b). However, in the only two station profiles available there is a tendency for $Ri(z)$ to decrease with depth, especially in Station 6. In interpreting these Richardson numbers it has to be kept in mind that the vertical resolution of $Ri(z)$ is low owing to a bin size of 4 m in

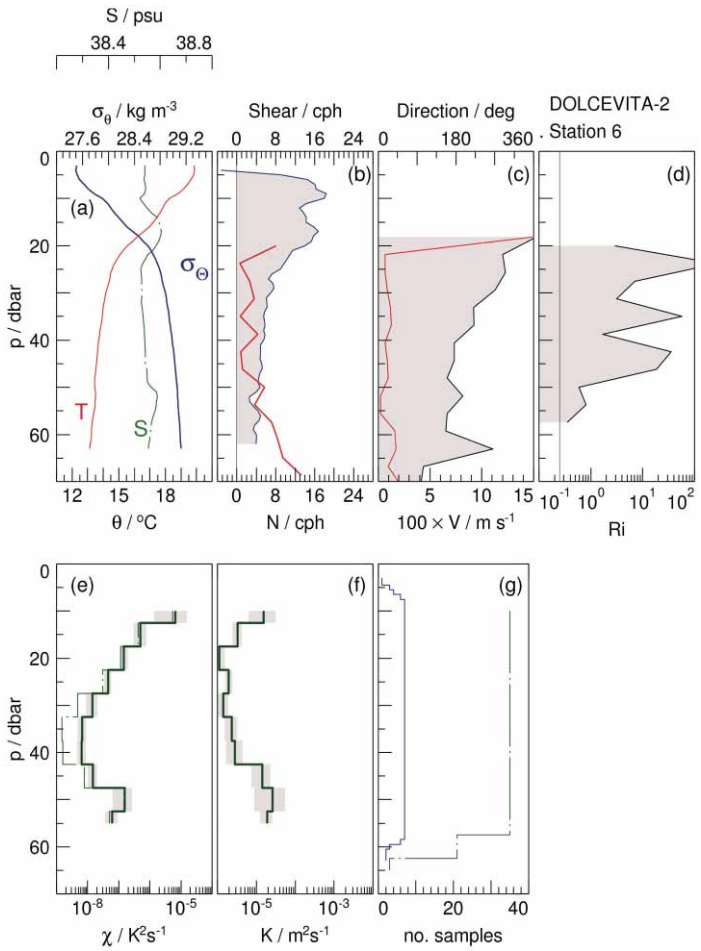

Figure 8. Mean Station 6 profiles: see Fig. 6.

the ADCP velocity measurements, the derivation of shear through differencing, and the averaging of a large number of ADCP pings. Hence the observed $Ri > 1/4$ does not exclude actual flow instability on unresolved small vertical scales, *e.g.* in relationship to smallscale internal waves.

c. Mesoscale Currents

The ocean currents observed from the *Dallaporta* in the depth range of 12–28 m are depicted in Fig. 11, which shows mesoscale variability of rather weak currents not exceeding 0.15 m s^{-1}. The velocity profiles of Stations 4–6 (Figs. 6c–8c) exhibit significant barotropic flow as shown by the limited depth variability of the current direction. Hence Fig. 11 is representative of

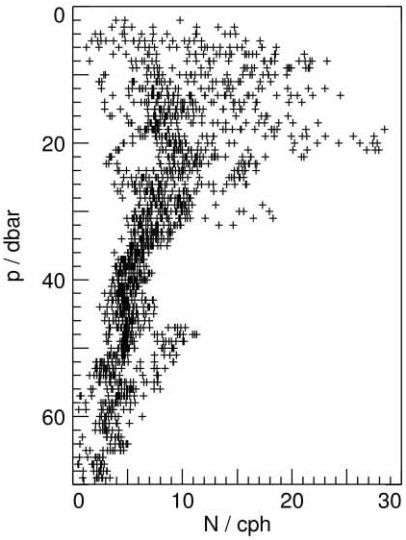

Figure 9. Individual stratification data computed over 2-m intervals from all *Dallaporta* CTD and SWAMP drops.

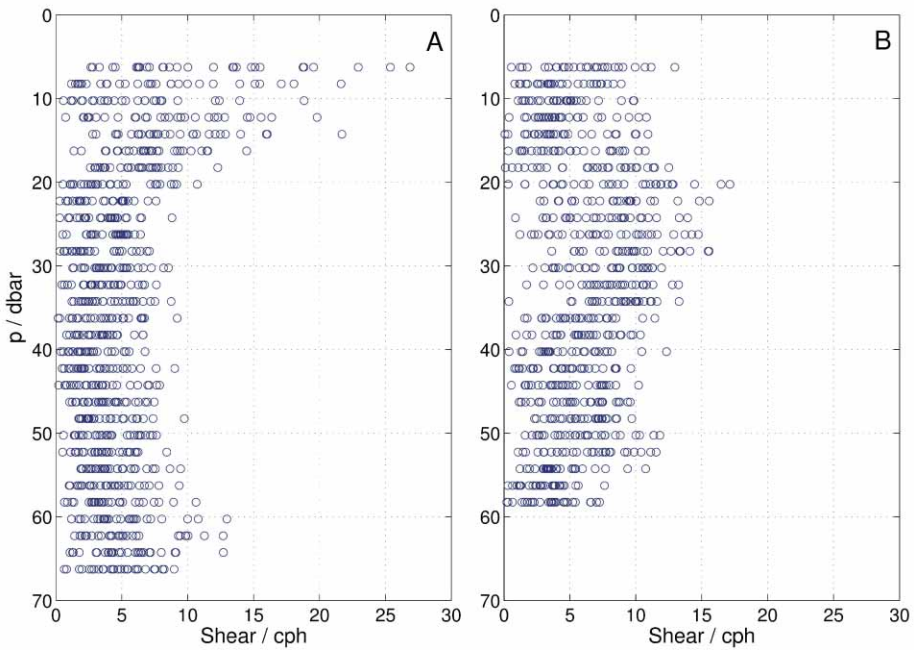

Figure 10. Hourly current shear for EACE moorings A and B and the time interval between 27-May-03 0800 UTC and 28-May-03 1200 UTC. Shear is defined in Section 2 and converted to cycles per hour for comparison with *N*.

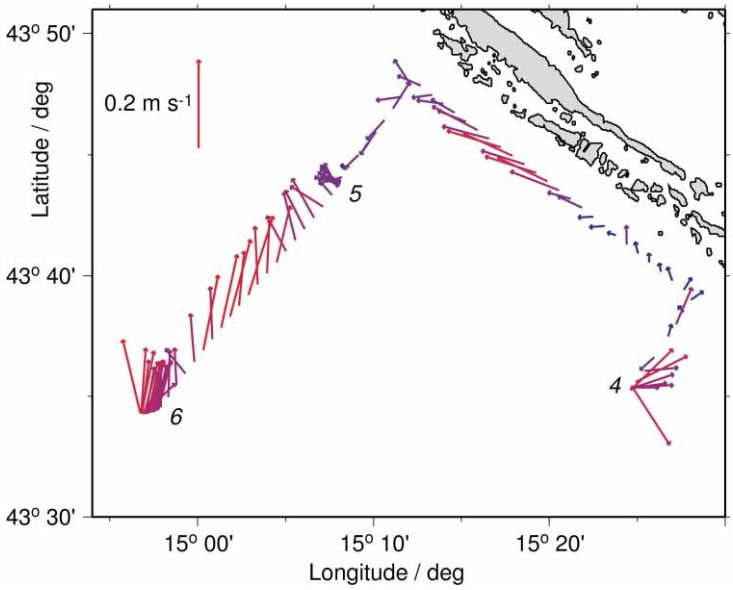

Figure 11. Current vectors at 12-28 m depth from the towed ADCP, 6-min averages. Station locations are indicated in italics.

the depth-averaged flow. The dominance of the barotropic over the baroclinic flow component is consistent with the finding of relatively weak shear as discussed above.

4. Mixing

The turbulent mixing characterized by ε, χ, K_h and K_ρ varied greatly with depth and at any one depth in our small data set as shown in Figs. 3–8. When all estimates of K_h are plotted together (Fig. 12), a simple pattern emerges. Disregarding depths shallower than 20 m and one large K_h at 30 m to be discussed below, values of K_h were all below 10^{-4} m^2 s^{-1}, many below 10^{-5} m^2 s^{-1}, and some as small as 10^{-6} m^2 s^{-1}. Relatively large eddy diffusivities partly exceeding 10^{-4} m^2 s^{-1} occurred at shallow depths of 10–25 m; K_h stayed below 3×10^{-5} m^2 s^{-1} at 30–40 m, and there was a general trend toward an increase of K_h with depth further below. This pattern of the depth variability of K_h corresponds with the elevated shear in the upper 20 m at EACE mooring A (Fig. 10A), and the small N below about 60 m in Fig. 9.

More specifically, the smallest eddy diffusivities appeared in Stations 1 (Fig. 3) and 6 (Fig. 8). All stations had comparatively large K_h at shallow depths, and all stations except 2 and 3 exhibit an increase in K_h with depth toward 60 m. The increase with depth of χ and K_h below 40 m in Station 6 (Fig. 8) is easy to interpret. This enhancement of mixing parallels an in-

crease with depth of shear and a corresponding decrease in Ri, which dropped below 1 below 50 m depth. This is the only case where the resolved shear and Ri appear to be related to the variations in mixing. In contrast, the strong increase in ε, χ, K_h, and K_ρ from 30 m depth to 10 m depth in Station 4 (Fig. 6) was paralleled by virtually constant shear and Ri.

The most eye-catching feature is the maximum of all turbulence variables near 30 m depth in Station 3 (Fig. 5) with $\varepsilon \sim 10^{-6}$ W kg^{-1} and $\chi \sim 10^{-5}$ K^2 s^{-1}. While this feature appears smeared out in the vertical in the station averages, individual drops show it to be a sharply defined, 4 m thick internal mixed layer (Fig. 13). The large measured dissipation rate and the pronounced thermal activity demonstrate that this was an actively *mixing* layer. As the stratification inside this layer was very close to neutral, the eddy diffusivity is undefined inside the mixed layer, and the corresponding data points at 30 m depth of Station 3 in Figs. 5e and 12 should be ignored.

The internal mixing layer of Station 3 is reminiscent of similar features found elsewhere in the oceans, some being attributed to shear-induced, persistent mixing related to internal near-inertial waves (Gregg et al., 1986; Hebert and Moum, 1994). As the ADCP had not yet been set up during Station 3, we are unable to examine the velocity structure associated with the internal mixed layer and to probe for the presence of near-inertial waves. However, the mixing time scale associated with the event is surprisingly short, of the order of a buoyancy period. Following Gregg (1987), the change

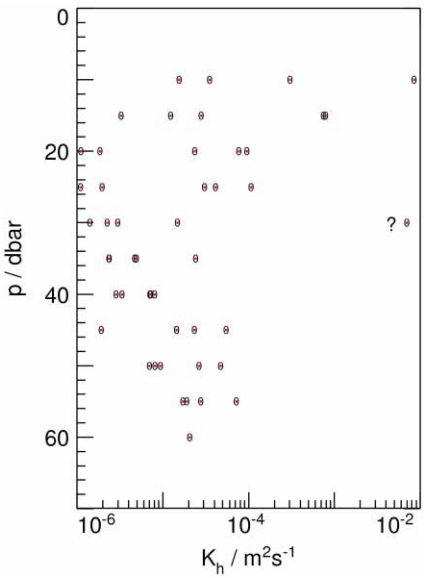

Figure 12. Eddy diffusivity of heat from all stations. The data point marked by »?« corresponds to the mixed layer depicted in Fig. 13, where the Osborn-Cox method is not applicable.

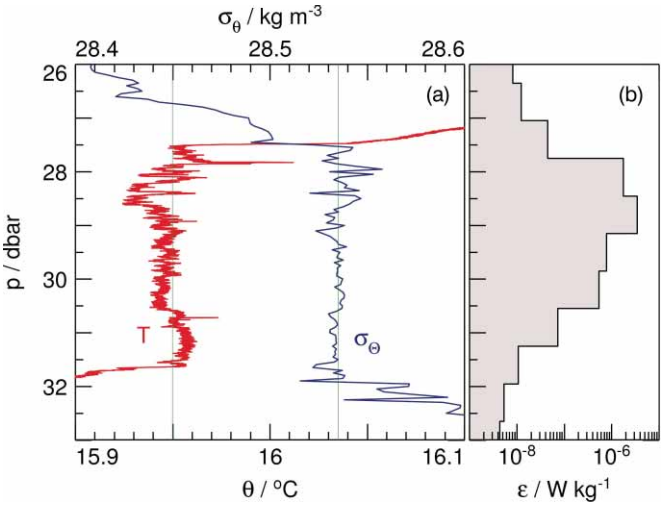

Figure 13. Internal mixed layer during Station 3 (drop 8091; 27-May-03 2231 UTC): (a) 256-Hz potential temperature and 5-cm average potential density from the micro-CTD sensors; (b) dissipation rate.

in potential energy density corresponding to creating a mixed layer of thickness h in a fluid of stratification N^2 is $\Delta E_p = N^2 h^2 / 12$ [J kg^{-1}]. Fig. 5 indicates $N = 6$ cph and $h = 4$ m. Equating the buoyancy flux that created the change in potential energy with the observed $\varepsilon = 7 \times 10^{-7}$ W kg^{-1} times a mixing efficiency of 0.2 leads to a mixing time scale of $\Delta E_p / (0.2\varepsilon) \approx 10^3$ s, or 17 minutes compared to a buoyancy period of 10 min.

Figs. 4c, 5c and 6e show estimates of the buoyancy Reynolds number. Most of the Re_b values are below 100 with few data reaching or exceeding 1000. This indicates moderate »activity« for the most part.

The graphs of χ, ε and K_h in Figs. 3–8 show statistical confidence limits computed by bootstrapping (Efron and Gong, 1983). These outline the effect on the mean of short-term variability within the observations. They are not related to longer-term averages.

5. Conclusions

In late May 2003 winds over the central eastern Adriatic were light, mixed layers were shallow, stratification was mostly strong, shear weak, and Richardson numbers were large. Below some near-surface enhancement and above weaker enhancement toward 60 m depth, turbulent mixing in a »mid-depth« range of 30–40 m was mostly weak, characterized by eddy diffusivities ranging from 10^{-6} m^2 s^{-1} to 5×10^{-5} m^2 s^{-1}. Much more intense mixing occurred in rare events, with eddy diffusivities being close to the literature values for the area.

The event-related maxima imply that a much larger set of observations than presented here is needed to characterize climatological averages of mixing rates and their variability. The finding also implies that mechanisms creating events of intense mixing deserve attention given that mean mixing rates may be largely determined by relatively few energetic events. Gregg (1987), for example, discusses the approximately lognormal statistics of ε and χ in the ocean and, in mixing events, distinguishes between highly transient »wisps« and longer-lasting »billows,« the latter often being related to the instability of persistent shear set up by near-inertial waves. We further note that current numerical circulation models do not resolve processes that create intense mixing events, such as near-inertial internal waves. In addition, turbulence closure schemes typically incorporated in numerical models are ignorant of the internal wave field. If models of the Adriatic circulation need to employ realistic levels of mixing, a renewed interest in observing oceanic mixing and its generating processes may well be required. We would be happy if this limited study could stimulate such interest.

Acknowledgments – This study was funded by the United States Office of Naval Research, contract ONR N0014-011-021. We are indebted to Dr. Stephen Murray for steering us toward the Mediterranean after the original destination of the effort, the Strait of Hormuz, became effectively off-limits because of security concerns. Funds for instrumentation were provided through the ONR DURIP program under contract N00014-98-1-0818. Dr. Craig Lee got us on board of the international DOLCEVITA project and was a big help all along. This project was initiated by Drs. Benoit Cushman-Roisin, Pierre Flament and Pierre Poulain. RSMAS technicians Mark Graham and Robert Jones prepared the instruments, organized the cruise logistics, and were as professional, hard-working and fun to be with as ever at sea and ashore. We thank them as well as the remainder of the *Dallaporta* science party, students Benjamin Jaimes de la Cruz, Marko Mlinar and Giuseppe Giacama. The director of the IRPEM Marine Fisheries Research Institute of the National Research Council of Italy, Dr. Antonio Artegiani, as well as Dr. Aniello Russo, Dr. Mauro Marini and other IRPEM employees went out of their way far beyond ordinary calls of collegiality in allowing us to store our instrumentation at the IRPEM in between the two DOLCEVITA cruises and in physically helping us to get them in and out of storage. The remarkable skills of a local truck and crane operator came especially handy. We further thank the operator of the *R/V G. Dallaporta*, Fritelli Maritime Group S.p.A., Signora Clara Vitorietti. We especially appreciate her patience in dealing with University of Miami lawyers. The *R/V G. Dallaporta* was commanded by Captain Silvano Argenti. Wind data and meteorological modeling results were supplied by the Hydrometeorological Institute of the Republic of Croatia. EACE was funded by the United States Office of Naval Research (grant 493264, administrated by the University of Washington) and the Croatian Ministry of Science and Technology. Drs. Vlado Dadić and Miroslava Pasarić were instrumental in EACE measurements and data analysis. Permission to work in the territorial waters of the Republics of Croatia and Italy is gratefully acknowledged, as is the assistance by the U.S. Department of State, Ms. Roberta Barnes and Ms. Elizabeth Tirpak.

References

Batchelor, G. K. (1959): Small-scale variation of convected quantities like temperature in a turbulent fluid, I, General discussion and the case of small conductivity. *J. Fluid Mech.,* **5**, 113–133.

Baumert, H., and H. Peters (2000): Second moment closures and length scales for stratified turbulent shear flows. *J. Geophys. Res.,* **105**, 6453–6468.

Efron, B., and G. Gong (1983): A leisurely look at the bootstrap, the jackknife, and cross-validation. *Am. Stat.,* **37,** 36–48.

Fleury, M., and R. G. Lueck (1994): Direct heat flux estimates using a towed vehicle. *J. Phys. Oceanogr.,* **24**, 801–818.

Gačić, M. (1972): On the characteristics of the eddy diffusion coefficient in the middle Adriatic (in Croatian). *Hidrogr. God.,* **70,** 105–129.

Gargett, A. E. (1985): Evolution of scalar spectra with the decay of turbulence in a stratified fluid. *J. Fluid Mech.,* **159**, 379–407.

Gargett, A. E., Osborn, T. R. and P. W. Nasmyth (1984): Local isotropy and the decay of turbulence in a stratified fluid. *J. Fluid Mech.,* **144**, 231–280.

Grbec, B., and M. Morović (1997): Seasonal thermohaline fluctuations in the middle Adriatic Sea. *II Nuovo Cimento,* **C20,** 561–576.

Gregg, M. C. (1987): Diapycnal mixing in the thermocline: A review. *J. Geophys. Res.,* **92**, 5249–5286.

Gregg, M. C. (1999): Uncertainties and limitations in measuring e and χ_t. *J. Atmos. Ocean. Tech.,* **16**, 1483–1490.

Gregg, M. C. and T. B. Meagher (1980): The dynamic response of glass rod thermistors. *J. Geophys. Res.,* **85**, 2779–2786.

Gregg, M. C., d'Asaro E. A., Shay T. J., and N. Larson (1986): Observations of persistent mixing and near-inertial waves. *J. Phys. Oceanogr.,* **16**, 856–885.

Hebert, D. and J. N. Moum (1994): Decay of a near-inertial wave. *J. Phys. Oceanogr.,* **24**, 2334–2351.

Jacobsen, J. P. (1927): Eine graphische Methode zur Bestimmung des Vermischungskoeffizienten im Meere. *Gerl. Beitr. Geophys.,* **16**, 404–412.

Lee, C. M. and M. Others (2005): Northern Adriatic response to a wintertime bora wind event. *Eos Trans. AGU,* **86(16),** 157.

Lueck, R. G., Huang, D., Newman, D. and J. Box (1997): Turbulence measurements with a moored instrument. *J. Atmos. Ocean. Tech.,* **14**, 142–161.

Malačič, V. (1991): Estimation of the vertical eddy diffusion coefficient of heat in the Gulf of Trieste (Northern Adriatic). *Oceanol. Acta,* **14**, 23–32.

Moum, J. N. (1996): Efficiency of mixing in the main thermocline. *J. Geophys. Res.,* **101**, 12,057–12,070.

Nash, J. D., Caldwell, D. R., Zelman, M. J., and J. N. Moum (1999): A thermocouple probe for high-speed temperature measurements in the ocean. *J. Atmos. Ocean. Tech.,* **16**, 1474–1482.

Orlić, M. (2003): Field phase of the East Adriatic Coastal Experiment completed. *EOS*, *Trans. AGU,* **84 (52)**, OS200, Ocean Sciences Supplement, Abstract OS52E–04.

Osborn, T. R. (1980): Estimates of the local rate of vertical diffusion from dissipation measurements. *J. Phys. Oceanogr.,* **10**, 83–89.

Osborn, T. R. and C. S. Cox (1972): Oceanic fine structure. *Geophys. Fluid Dyn.,* **3**, 321–345.

Peters, H. (1997): Observations of stratified turbulent mixing in an estuary. Neap-to-spring variations during high river flow. *Estuar. Coast. Shelf Sci.,* **45,** 69–88.

Peters, H., Gregg, M. C. and J. M. Toole (1988): On the parameterization of equatorial turbulence. *J. Geophys. Res.,* **93,** 1199–1218.

Peters, H., Gregg, M. C. and T. B. Sanford (1995): Detail and scaling of turbulent overturns in the Pacific Equatorial Undercurrent. *J. Geophys. Res.,* **100,** 18,349–18,368.

Rohr, J. J., Itsweire, E. C., Helland, K. N. and C. W. Van Atta (1988): Growth and decay of turbulence in a stably stratified shear flow. *J. Fluid Mech.,* **195,** 77–111.

Saint-Guily, B. (1965): Diffusion thermique turbulente au niveau de la pycnocline. *Rapp. Proc.-Verb. Reun. CIESMM,* **18/3**, 865–869.

Schmidt, W. (1917): Wirkungen der ungeordneten Bewegung im Wasser der Meere und Seen. *Ann. Hydrogr. Marit. Meteorol.,* **45,** 367–381, 431–445.

Smyth, W. D., Moum, J. N. and D. R. Caldwell (2001): The efficiency of mixing in turbulent patches; Inferences from direct numerical simulations and microstructure observations. *J. Phys. Oceanogr.,* **31,** 1969–1992.

Supić, N., Orlić, M. and D. Degobbis (1997): Small-scale spatial variability of surface heat flux over the northern Adriatic. *Period. Biol.,* **99,** 169–179.

Vilibić, I., Grbec, B. and N. Supić (2004): Dense water generation in the north Adriatic in 1999 and its recirculation along the Jabuka Pit. *Deep-Sea Res. I,* **51**, 1457–1474.

Winters, K. B. and E. A. D'Asaro (1996): Diascalar flux and the rate of fluid mixing. *J. Fluid Mech.,* **317,** 179–193.

Yamazaki, H. and T. R. Osborn (1993): Direct estimation of heat flux in the seasonal thermocline. *J. Phys. Oceanogr.,* **23,** 503–516.

Zore-Armanda, M. (1963): Les masses d'eau de la mer Adriatique. *Acta Adriatica,* **10/3**, 1–93.

Appendix: Detail of Data Reduction and Uncertainties

A Seabird 911+ CTD was used on Stations 1 and 5 in a quasi-free fall mode with buoyancy attached to the CTD frame. The sensors of this »regular« CTD as well as the SeaBird sensors of SWAMP were calibrated by the manufacturer. However, the conductivity sensor of SWAMP had drifted while the instrument was in storage, and thus we added a constant 0.3 psu to the SWAMP CTD salinity. After this, the 911+ CTD and SWAMP *TS* relationships of Station 1 matched each other. In consequence of the sensor drift the SWAMP CTD salinity may carry a systematic bias of about ± 0.03 psu.

The SWAMP thermistor and micro-conductivity sensors were calibrated linearly against their CTD counterparts. A single calibration holds for the thermistor for all drops with an accuracy of ± 0.03 °C and an RMS electronic noise of about 0.003 K (see Fig. 13a). In contrast, the micro-conductivity had to be individually calibrated for each drop, but even so the micro-C drifted considerably during some drop segments. Unfortunately, the pump of the SWAMP SeaBird *TC* duct was not turned on during Station 3, and thus stratification information had to be taken from the micro-*T* and micro-*C* sensors. The corresponding salinity, lacking proper calibration for each drop, is rather uncertain and thus not shown in Fig. 5a. Fortunately, depth-variations of S were quite small such that $\sigma_\theta(z)$ and $N(z)$ of Station 3 are still acceptably accurate. For this study the accuracy of vertical stratification gradients is important while small biases in the stratification variables are not crucial.

The evaluation of the microscale shear data in terms of ε follows Peters (1997) and a long line of sources cited therein. It may suffice to mention here that these data are highly sensitive to mechanical noise and that noise and signal are separated in the spectral domain. For this study, additional routines were written that identify segments of elevated signal in the auxiliary accelerations sensor of SWAMP, which correspond to elevated mechanical noise, and flag the corresponding ε data. The data being analyzed herein were gathered while the operations of our small science party on the *Dallaporta* were still in the mode of setting up, shaking down, and gaining experience. It has to be understood on this background that ε data from Stations 1 and 6 suffer from mechanical noise such that they are not shown in Figs. 3 and 8. With this, this paper relies principally on χ rate in quantifying turbulent mixing.

Thermal dissipation rates are relatively insensitive to mechanical noise as they respond only to sensor displacement rather than to acceleration. For the determination of χ, noise was separated from signal in the spectral domain, a noise floor invariant in time being established by studying many temperature gradient spectra. In these, the noise floor follows from white noise modified by the various filters employed in the analog electronic section of SWAMP, principally an analog differentiator and an anti-aliasing filter. Temperature gradient signals were used to a maximum of 60 Hz, and the spectrum was corrected for the temporal response of the thermistor following Gregg (1999) and Nash et al. (1999), with further reference to Lueck et al. (1977), Gregg and Meagher (1980), and Fleury and Lueck (1994). The correction assumes a double pole response $H(f) = [1+(f/f_c)^2]^2$, where f is the frequency and the nominal cut-off frequency f_c marks the 6 db point of the response function. We assume $f_c = 32\ w^{0.32}$ with fallrate w in m s^{-1}. With a fallrate of 0.5 m s^{-1}, the 6 db point of the temporal response is at 26 Hz, and thus spectral corrections are mostly large. The corresponding time constant is 6 ms. As the instrument and its sensors were lost at sea, it was not possible to experimentally determine τ for the individual thermistor used after the cruise, and thus the principal source of uncertainty in χ is rooted in the unknown temporal thermistor response.

In order to further explore this effect we conducted a sensitivity study. Noting that the fallrate of SWAMP of just under 0.5 m s^{-1} varied little, we determined χ and K_h with $f_c = 21.3w^{0.32}$, which, following experience with FP07 thermistors, characterizes the slow end of plausible thermistor responses. The corresponding χ are larger than their counterparts depicted in Figs. 3–8 by factors that increase with χ itself, typically being smaller than 50% but rising to factors of 2–3 at large χ.

At small χ temperature gradient spectra tended to drop into the noise without resolving the diffusive cut-off. We corrected χ for unresolved temperature variance on the basis of the Batchelor (1959) spectrum. The magnitude of this correction was generally small and significant only in some segments

of small χ, *e.g.* near 40 m depth in Fig. 8d. Figs. 3–8 show both corrected and uncorrected χ. In cases of weak mixing such as this in Fig. 8d, the actual spectra tended not to follow the Batchelor (1959) shape, a finding not unanticipated (Gargett, 1985). The uncorrected χ provides a lower bound for the true χ. Hence, in the case of Station 6, 33–42 m depth, the true K_h may have been smaller than the value plotted in Fig. 8e by factors of 3–5.

Above, we state that the maxima of K_h and K_ρ at 30 m depth in Fig. 5e should be ignored because the vertical temperature and density gradients vanish inside the internal mixed layer observed at that site. This statement emphasizes limitations in the local applicability of the Osborn-Cox method, equation (1), and the Osborn method, equation (2). Respectively, the mean vertical temperature gradient and mean vertical density gradient, *i.e.* N^2, need to be well-defined. The Osborn-Cox method can fail in regions of complex TS variations and weak and variable $\partial T/\partial z$. The large excess of K_h over K_ρ at 20–25 m in Station 4 (Fig. 6g) is explained by such condition.

SAŽETAK

Turbulentno miješanje u srednjem Jadranu tijekom proljeća

Hartmut Peters i Mirko Orlić

U svibnju 2003. godine prikupljen je u srednjem Jadranu nevelik niz podataka kojim je dokumentirano turbulentno miješanje u površinskom sloju te stratifikacija i strujanje. Budući da su vjetrovi bili slabi, površinski izmiješani sloj dosizao je najviše do dubine od 10 m, često i manje. Vodeni stupac ispod tog sloja bio je uglavnom jako stratificiran, uz prisutnost ostataka ranijih izmiješanih slojeva koji su dijelom ponovno stratificirani. Struje su bile malih brzina na srednjoj skali, s time da je barotropna komponenta bila značajna. Slabo smicanje i dobro izražena stratifikacija doprinosili su velikim iznosima Richardsonovog broja. Ispod sloja debljine 10–20 m u kojem je miješanje bilo pojačano, koeficijenti turbulentnog miješanja uglavnom su bili malih iznosa, između 10^{-6} m^2 s^{-1} i 5×10^{-5} m^2 s^{-1}. Međutim, u nekoliko su slučajeva opažene znatno veće vrijednosti.

Ključne riječi: mikrostruktura, turbulencija, Jadran

Corresponding author's addresses : H. Peters, Rosenstiel School of Marine and Atmospheric Science, University of Miami, 4600 Rickenbacker Causeway, Miami, FL 33149-1098, USA, e-mail: hpeters@rsmas.miami.edu;
M. Orlić, Department of Geophysics, Faculty of Science, University of Zagreb, 10000 Zagreb, Horvatovac bb, Croatia, e-mail: orlic@irb.hr.